5
Improved Odour Detection through Imposed Biomimetic Temporal Dynamics

Tim C. Pearce[1], Manuel A. Sánchez-Montañés[2], and Julian W. Gardner[3]

[1] Department of Engineering, University of Leicester, Leicester LE1 7RH, United Kingdom
[2] Escuela Politécnica Superior, Universidad Autónoma de Madrid, Madrid 28049, Spain
[3] School of Engineering, University of Warwick, Coventry CV4 7AL, United Kingdom

Abstract. We discuss a biomimetic approach for improving odour detection in artificial olfactory systems that utilises temporal dynamical delivery of odours to chemical sensor arrays deployed within stationary phase materials. This novel odour analysis technology, which we have termed an artificial mucosa, uses the principle of "nasal chromatography"; thus emulating the action of the mucous coating the olfactory epithelium. Temporal segregation of odorants due to selective phase partitioning during delivery in turn gives rise to complex spatio-temporal dynamics in the responses of the sensor array population, which we have exploited for enhanced detection performance. We consider the challenge of extracting stimulus-specific information from such responses, which requires specialised time-dependent signal processing, information measures and classification techniques.

5.1 Three Key Mechanisms for Discrimination of Complex Odours in Chemical Sensor Arrays

The detection capability of chemical sensor array systems is limited by both sensor noise and the degree to which response properties can be made stimulus specific and diverse across the array (Pearce & Sánchez-Montañés 2003). Two main mechanisms for odour discrimination in artificial olfactory systems have been exploited so far:

1. To generate diverse responses, sensors within the array are typically selected to produce an ensemble of complementary wide spectrum broad tunings to the different volatile compounds of interest. Given sufficient diversity in these tunings, a spatial fingerprint of a particular complex odour should be generated across the array that is sufficiently stimulus specific to overcome noise limitations, and may then be used as part of a pattern recognition scheme for odour discrimination (Pearce *et al.* 2003). In this case, the role of time is not considered explicitly, but rather the magnitudes of the responses across the array, which is the classical method of odour classification in artificial olfactory systems.

A. Gutiérrez and S. Marco (Eds.): Biologically Inspired Signal Processing, SCI 188, pp. 75–91.
springerlink.com

2. Depending upon the choice of chemosensor technology and the compounds under investigation, it is possible that the chemosensor dynamics themselves can also depend on the compounds present in the mixture (Albert *et al.* 2002), leading to an additional dimension of temporal variation which can be exploited for the purposes of discrimination. Such differences have previously been exploited to improve discrimination performance (e.g. Llobet *et al.* 1997, White and Kauer 1999).

In biological olfaction, on the other hand, the temporal dimension is known to play a much more central role in the processing of olfactory information (Schoenfeld and Cleland 2006) than has thus far been considered in machine olfaction research. For instance, the timing and dynamics of the sniffing process are known to be important (Kepecs *et al*. 2006), which appears to be well matched with the timing of neural processing mechanisms in the olfactory bulb, as emphasised by many modellers (*e.g.* Brody and Hopfield, 2003). Looking at the overall processes involved in olfactory perception, this may be viewed as an exquisitely timed and orchestrated sequence of odorant inhalation, odorant partitioning and absorption, olfactory neuron timing responses mediated by calcium dynamics, the arrival and complex integration of spikes at glomeruli and the finely balanced dynamics of excitation and lateral inhibition in the bulb. When building biomimetic olfactory systems, therefore, we should consider carefully the timing and temporal aspects of the delivery and processing of sensory information.

By considering the role of timing of odorant delivery in biological olfaction (Rubin & Cleland 2006), we have recently built a novel machine olfaction technology, termed an "artificial olfactory mucosa", which demonstrates clearly a third principle of odour discrimination in artificial olfactory systems:

3. By creating a temporal profile of odour delivery to the different sensors within the array that is stimulus specific, we may provide additional response diversity. This is achieved by deploying chemical sensor arrays within stationary phase materials that impose the necessary stimulus-dependent spatio-temporal dynamics in sensor response; we have recently shown that this approach aids complex odour discrimination (Gardner *et al.* 2007). This concept is very different to that embodied within classical electronic nose systems that are usually designed to control the exposure of the stimulus as a square pulse, whose temporal properties are independent from the nature and chemical composition of the stimulus. Instead, we exploit such differences to generate additional discrimination capability in the device.

5.2 An Artificial Olfactory Mucosa for Enhanced Complex Odour Analysis

This third discrimination mechanism uses the physical positioning of a series of broadly tuned sensors along the length of a planar chromatographic channel (analogous to the thin mucous coating of the nasal cavity) which gives rise to more diversity in the temporal properties in the sensor signals (retentive delay and profile). Figure 5.1 shows the basic architecture of the artificial mucosa concept and its biological counterpart. A complex odour pulse travelling in the mobile carrier phase

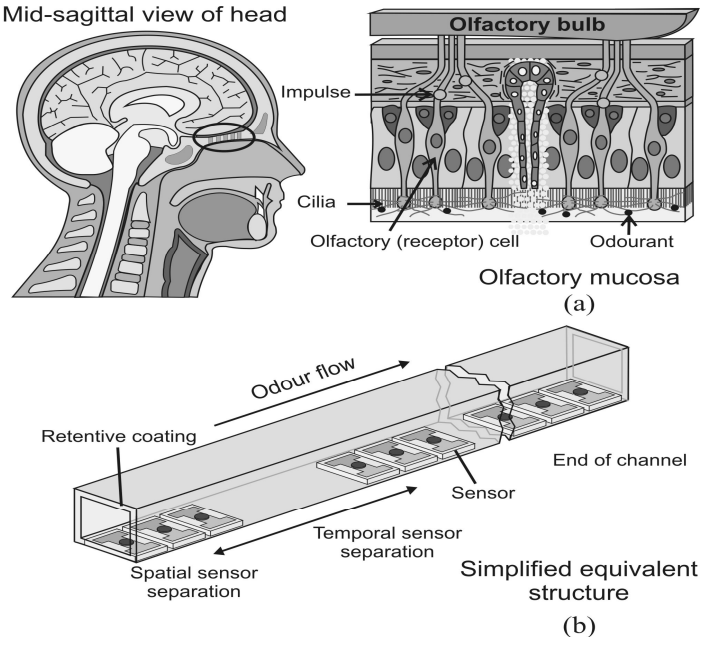

Fig. 5.1. a) Sagittal head view showing the main sections of the olfactory mucosa and subsequent neural processing. Odour molecules during inhalation selectively partition into a mucous layer covering specialized dendritic cilia from olfactory receptor neurons in the nasal epithelium. Odours interact with receptor proteins embedded within the cilia membrane to mediate ORN calcium dynamics, ultimately leading to the generation of additional action potentials (*impulses*). These action potentials are transmitted to the olfactory bulb via axonal projections where these are processed to interpret complex odour information. **b)** An artificial mucosa that relies on similar principles of odorant partitioning to its biological counterpart. The chemosensor array is deployed inside a microchannel coated with a stationary phase material (*retentive coating*) that has selective affinity to the different compounds with a complex mixture. By introducing a pressure difference across the microchannel odour flow may be pulsed within the microchannel, giving rise to segregation in odour components that is compound specific. (Reprinted with permission by Royal Society, London).

inside the artificial mucosa gives rise to selective partitioning of components causing the odour components to travel at different speeds into the mucosa, leading to a kind of chromatographic effect. Depending upon the degree of affinity of each component compound for the retentive layer, this will be found within the mobile (carrier) and stationary (retentive layer) phases in compound specific ratios. The retention of each odour component in the stationary phase acts to retard the progress of the pulse for that compound through the mucosa, leading to segregation in the components of the stimulus in accord with the well understood principles of gas capillary column chromatography (Purnell 1962).

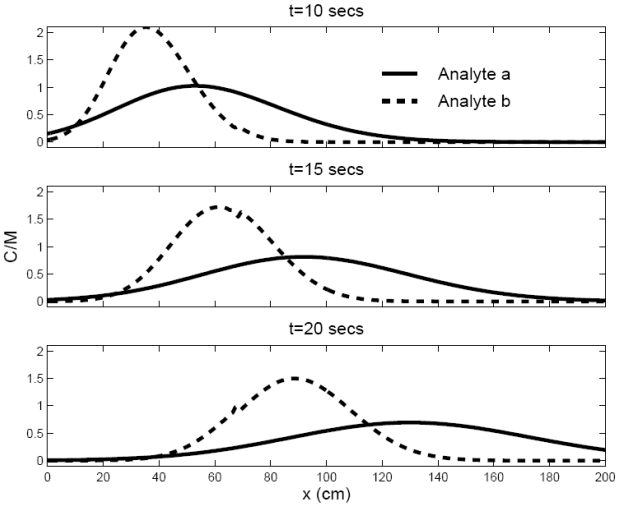

Fig. 5.2. Numerical solutions of an analytical model for concentration for two compounds *a* and *b* at different positions, *x*, within the artificial mucosa. Carrier velocity inside the micro-channel is 15 cm s^{-1}, mass distribution coefficients $k_a = 1$ and $k_b = 2$, and effective diffusion coefficients $D'_a = 50$ cm^2 s^{-1} and $D'_b = 10$ cm^2 s^{-1}. Pulse duration at inlet ("sniff time"), $t = 5$ s.

We will see that this arrangement provides an important additional mechanism for odour discrimination, since depending upon their location in the mucosa, each sensor will receive a particular sequence of single or subsets of compounds within a complex mixture over time, which is a function of the stimulus composition. It is important to understand and accurately describe the transportation of odour compounds within the artificial mucosa in order to verify the experimental results, as well as provide the basis for an optimisation procedure of its design for complex spatiotemporal chemical sensing. We have developed both finite element and analytical models for this purpose. Figure 5.2, for example, shows the numerical solution of our analytical model of local concentration profiles within the micro-channel for two compounds, *a* and *b*, injected simultaneously at the inlet as they progress through the device. We see a clear separation between the two compounds that increases over time and depends directly upon the difference in partition coefficients and so is compound and stimulus specific. In both cases the dispersion, which determines the degree of overlap, depends upon the effective diffusion coefficient while the velocity of propagation through the mucosa depends upon the effective partition coefficient between the compound and the stationary phase deployed.

Differential sorption of compounds within the artificial mucosa gives rise to a temporal fingerprint in the chemosensor response which is sensitive to the concentrations and presence of different compounds. The important aspect here that is distinct from previous techniques exploiting the temporal dimension is that the delivery of the stimulus itself becomes specific to the compound(s) being delivered, which imposes

additional diversity in the array responses. We have shown experimentally (Gardner *et al.* 2007) that deploying chemical sensor arrays within stationary phase materials in this way imposes stimulus-dependent spatio-temporal dynamics on their response, thereby aiding complex odour discrimination. We will also show theoretically at the end of this chapter that using both spatio-temporal responses (all three discrimination mechanisms) will always provide better detection performance than using spatial information alone (the first discrimination mechanism).

5.2.1 Artificial Olfactory Mucosa Fabrication

The artificial mucosa was constructed by mounting discrete polymer/carbon black composite chemoresistive sensors (40 devices of 10 different composites) on a printed circuit board (PCB) base sealed with two different polyester lids (with and without stationary phase coating, which we refer to here as the coated and uncoated mucosa) within which a serpentine microchannel was machined. Once sealed, this composite structure was injected with Parylene C ,as the absorbent stationary phase material, deposited using a commercial evaporation technique (PDS 2010 Labcoater^{TM} 2, Specialty Coating Systems, Indianapolis, USA). Each sensor chip was 2.5 mm × 4.0 mm in size and comprised a pair of thin co-planar gold electrodes on a SiO_2/Si substrate with an electrode length of 1.0 mm and an inter-electrode gap of 75 μm. Additional fabrication details are provided elsewhere (Gardner *et al*. 2007).

5.2.2 Chemical Sensor Behaviour within the Artificial Mucosa

In order to demonstrate the effect of the stationary phase material within the artificial olfactory mucosa, we tested rectangular pulses of simple odorants (toluene and ethanol) with the microchannel both coated and uncoated – Figure 5.3 shows the normalised results. In both cases, the sensor closest to the inlet of the microchannel (S1) shows a rapid onset time relative to that seen at the sensor towards the outlet (S39), which is due to the transport time for the odour pulse ("sniff"). However, in the uncoated case (Figure 5.3a), we see that the temporal response of the outlet sensor is not stimulus specific in time for ethanol and toluene after normalization. Thus, the uncoated mucosa adds no additional information in time, since within the limits of sensor noise, the outlet sensor is only able to discriminate between the two simple compounds based upon its response magnitudes – *i.e.* using the first mechanism of discrimination. Of particular note here is the broadening of the response signal in time with increasing sensor distance from the inlet, which is also observed in the responses of identical sensors placed at different locations along the channel. This is predominantly due to diffusion broadening of the odour as it travels along the micro-channel. Since the diffusion coefficient in air varies very little for different odour ligands, diffusion broadening, in itself, is not a particularly effective means of imposing stimulus dependent response diversity in artificial olfactory systems. We will see that selective partitioning can play a much more important role.

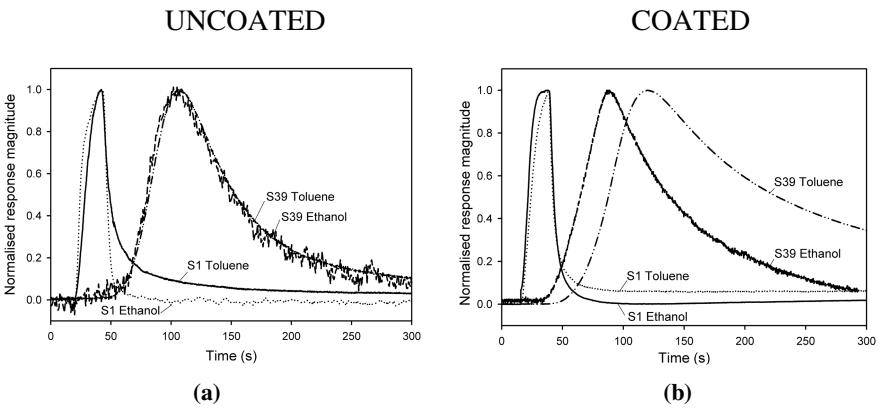

Fig. 5.3. Comparison of normalized chemosensor responses for an uncoated and coated artificial olfactory mucosa. **a)** Uncoated mucosa. Responses of sensor S1 (PEVA sensor material composite) close to the inlet and S39 (PCL sensor material composite) close to the outlet of the microchannel. **b)** Responses from the same sensors in the coated mucosa. (Reprinted with permission by Royal Society, London).

The uncoated responses of the inlet sensor also show some differential response that is stimulus dependent, which is most likely due to the kinetics of the ligand/sensor interaction rather than the mucosa properties – an example of the second discrimination mechanism discussed in Section 1 due to differential ligand/sensor temporal interactions.

In the coated case (the normal operational mode of the artificial mucosa - Figure 5.3b), the response of the outlet sensor after normalization shows very different temporal responses that are strongly stimulus specific. Here we see a clear additional latency in the onset of the response and also its duration is much longer, which is clearly due to spatio-temporal stimulus dynamics imposed by the coated mucosa when we compare to the uncoated case. This stimulus dependent difference in

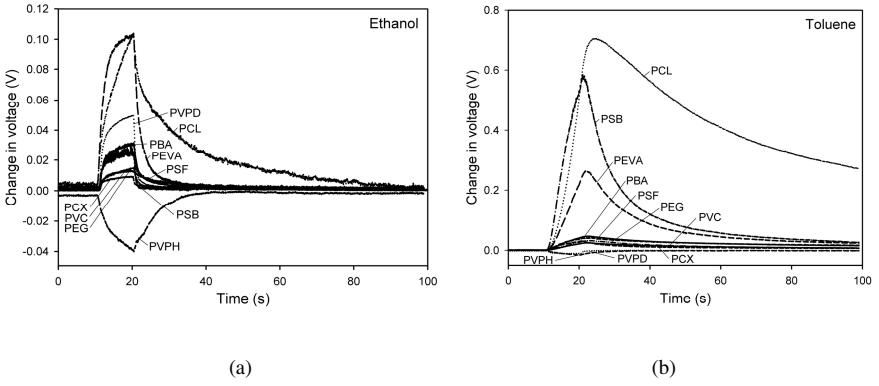

Fig. 5.4. Response of different types of sensors responding to a 10 s pulse of simple analytes. Sensor responses to **a)** ethanol vapour, and **b)** toluene vapour in air. (Reprinted with permission by Royal Society, London).

the outlet sensor response, demonstrates clearly the additional third mechanism for discrimination which we have produced through the use of selective coatings in our artificial mucosa design and believe to be analogous to odorant air/mucus interaction in the biological olfactory system. Figure 5.4 shows the diversity in the sensor responses for the different composite materials we have used within the artificial mucosa device. The ensemble response clearly shows a wide diversity that is strongly stimulus specific, both before and after normalisation. This additional temporal diversity due to selective partitioning is a powerful means for introducing additional discrimination capability to chemical sensor arrays for complex odour analysis.

5.3 Exploiting Temporal Responses in the Artificial Mucosa

The three mechanisms for discrimination in artificial olfactory systems are not mutually exclusive. Rather, as appears to be the case in biology, we may exploit differential responses due to diverse sensor tunings (first mechanism), ligand/sensor kinetic dependencies (second mechanism), and imposed spatio-temporal dynamics in the stimulus delivery (third mechanism) simultaneously. Making these three mechanisms for discrimination cooperate in tandem and in a selective way is, we believe, the key to building new generations of artificial olfactory systems that may begin to approach the impressive selectivity and broad range sensitivity found in biological systems.

In order to take advantage of the rich diversity of temporal responses created by the artificial mucosa we must analyse them with suitable signal processing and classification strategies, i.e. techniques that are time dependent. One approach is to again look to the biology for the principles involved in processing such spatio-temporal signals (Pearce 1997).

5.3.1 Olfactory Bulb Implementations for Spatiotemporal Processing of Odour Information

A large number of olfactory receptor neurons (ORNs) constitute the front-end of the olfactory system, being responsible for detecting airborne molecules. Cilia of the ORNs protrude into the olfactory mucosa (Figure 5.1), where they come in contact with molecules that are transported by the nasal air flow. On the surface of the cilia, odorant receptors bind odorant molecules with a broadly tuned affinity. When a receptor binds with an odorant molecule, it triggers in its ORN a biochemical cascade that eventually causes the membrane potential of the ORN to change, potentially leading to the generation of action potentials (Mori *et al.* 1999).

In vertebrates, ORNs project their axons into the olfactory bulb, terminating into spherical neuropils called glomeruli, where they connect onto the dendrites of mitral and tufted (M/T) cells. Experimental data indicate that each glomerulus receives the axons of only ORNs that express the same type of receptor, while any M/T cell sends its apical dendrite into one glomerulus only. Inhibitory neurons of the olfactory bulb form reciprocal contacts with many M/T cells via granule cells, thus forming together a complex network that appears to constitute the first stage of olfactory information processing. The output of the M/T cells is also relayed to higher brain areas (Mori *et al.* 1999).

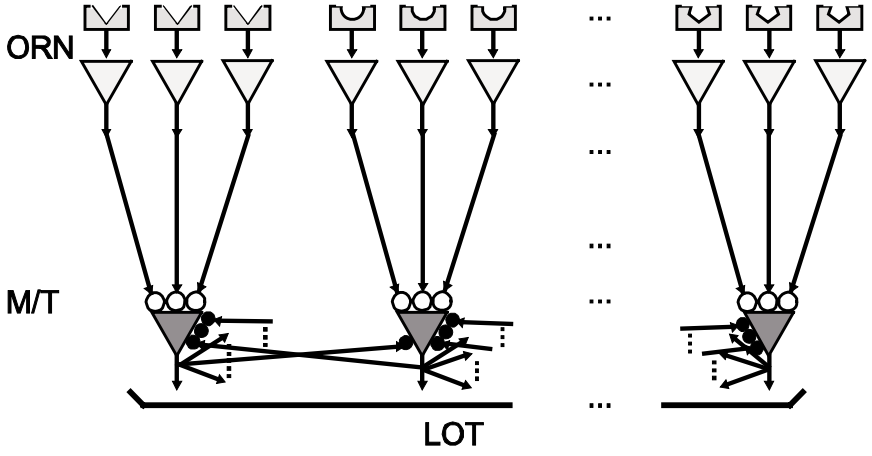

Fig. 5.5. A schematic diagram of the olfactory bulb neuronal model architecture which we have implemented in programmable logic (Guerrero and Pearce 2007) and aVLSI (Koickal *et al.* 2007) for real-time odour signal processing, showing receptor and principal neurons (triangles) and synapses (circles: unfilled – excitatory, filled – inhibitory). There are 25 M/T cells in total and 75 ORNs. M/T: mitral/tufted cells, ORN: olfactory receptor neurons. LOT: lateral olfactory tract.

Figure 5.5 shows the overall schematic of our network model for spatio-temporal odour signal processing (only showing three types of receptor input for the sake of clarity). The diagram has been drawn representing every computational element with an individual device, rather than adopting a biologically realistic representation. Chemosensors themselves are represented by irregular polygons at the top of the diagram which may be placed within the artificial mucosa to generate additional temporal diversity in their responses – polygons of the same shape represent sensors of the same type. Since the firing rate produced by ORNs is limited to approx. 1 kHz, we use a sigmoidal squashing function to condition the chemosensor signals before using it to drive the olfactory bulb (OB) model.

In our model, any ORN receives input from only one chemosensor/receptor type, and any chemosensor only projects to one ORN. The outputs of the ORNs feed into the respective ORN-M/T synapses (circles). The outputs of the synapses that receive input from ORNs converge a single M/T cell, where they are summed linearly. This represents the operation of glomeruli in the olfactory system. The output of any glomerulus feeds into one respective M/T cell. Because the signals from sensors of the same type are fed forward through neural elements to a single M/T cell, the network presents an evident modular structure, each module being defined by a different type of sensor, in a way that resembles the glomerular organization of the olfactory bulb. Every M/T cell projects to every other M/T cell through one of the M/T-M/T inhibitory synapses (filled circles).

The neurons themselves have been modelled as integrate-and-fire units. Below the threshold V_θ, the dynamics of the "membrane" potential $V(t)$ of the IF neuron are defined by the equation

$$\frac{dV(t)}{dt} = -\frac{V(t)}{RC} + \frac{I(t)}{C} \tag{5.1}$$

where t is time, R and C are, respectively, the membrane resistance and capacitance, and $I(t)$ is the total input current to the neuron. The membrane rest potential is conventionally set equal to the value zero. The membrane time-constant τ_m is given by RC (τ_m = 10 ms is used throughout as a biologically plausible value). The terms contributing to $I(t)$ are due to sensor responses if the neuron is a ORN, and to ORNs and lateral interactions if the neuron is a M/T cell. If the potential $V(t)$ reaches the threshold value V_θ, it is immediately reset to the afterhyperpolarisation value V_{ahp} and an action potential is produced as output of the neuron. Since we do not explicitly consider the role of adaptation in the model at this time, we set the threshold V_θ to be equal and fixed for all ORN and M/T cells.

The model also includes dynamical synapses based upon first order dynamics. In this case, currents generated by a synapse in response to a spike train is through an exponential decay over multiple spike inputs occurring at times (t_1, t_2, . . ., t_j , . . . t_l) to give the dendritic current

$$I(t) = w \sum_{j=1}^{l} H(t - t_j) \exp\left\{ -\frac{t - t_j}{\tau_{i;e}} \right\}, \tag{5.2}$$

where w specifies the weight or efficacy, $H(.)$ is the Heaviside function and $\tau_{i;e}$ is the synaptic time constant of either inhibitory or excitatory synapses. We choose a value of 4 ms for excitatory synapses, and 16 ms for GABA mediated inhibitory synapses.

The weights of the M/T-M/T synapses are defined so as to endow the network with associative properties (cf., e.g., Amit 1992 for general definitions), although it is not known whether the biological counterpart does perform this kind of processing. This lateral connectitivity represents dendrodendritic mitral/tufted and granule cell interactions in the external plexiform layer of the bulb, which are known to be important in mediateing odour memory (Hildebrand and Shepherd, 1997). The network learns odorants by modifying the weights of the M/T-M/T synapses according to a Hebbian learning rule, during a training stage. The activity of a given neuron i by means of its firing rate v_I (defined by a temporal average of spikes, hence, the mean firing rate v is the number of spikes $n_{sp}(t)$ that occur in the time T, $v = n_{sp}(T) / T$, where the v is expressed in Hz). The synaptic weight change is then given by the equation

$$\delta w_{ij} = \alpha \cdot v_i \cdot v_j, \tag{5.3}$$

where v_i and v_j are the firing rates of the postsynaptic and presynaptic cells respectively, and α is a learning parameter, such that α > 0. Since the spatial dependence of granule-mitral cell interactions is not fully understood, we choose the lateral weights, w_{ij} to be random before training.

Given a learnt Odour A, an indicator function of all M/T cell firing rates can be defined

$$f = k \frac{\mathbf{d}^{\mathrm{T}} \mathbf{a}}{\|\mathbf{d}\| \|\mathbf{a}\|}, \tag{5.4}$$

that indicates to which degree the network output is currently representing that particular odorant. Here **d** and **a** are vectors of the M/T cell population firing rates after training in response to the currently presented odour D and previously presented target Odour A. The indicator function is normalised by the magnitude of these vectors so that this may be interpreted as a correlation between **d** and **a**, scaled by k, which is kept constant for all indicator functions**.** Thus, when a previously learnt odorant is presented, its corresponding indicator function should assume a relatively large positive value.

We have implemented this spatio-temporal olfactory bulb network in both programmable logic (Guerrero & Pearce, 2007, Guerrero-Rivera et al., 2006) and in analogue VLSI technology (Koickal *et al.*, 2007) for the purposes of real-time processing for artificial mucosa. Such recurrent spiking neuronal models have been shown to exhibit Hopfield-like attractor based dynamical behaviour. The asymmetric nature of the connectivity in our model gives rise to a richer variety of dynamical behaviours than in the symmetric Hopfield case (Li and Dayan, 1999). Such networks have been shown in a variety of contexts to be sensitive to temporal properties in their input, for instance, temporal sequence processing (Wang 2003). We next show that the network is capable of supporting odour classification and odour compound detection in varying backgrounds.

A. Odour Classification

In order to demonstrate the classification properties of the OB model, the same network was subjected to two arbitrary but constant input patterns (that we term 'Odour A' and 'Odour B'), representing the receptor response to distinct odours at the input.

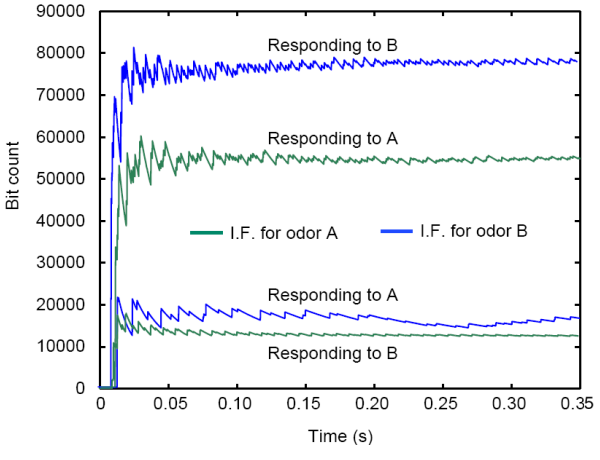

Fig. 5.6. Indicator functions for the odour classification task. The same network is trained to 2 odours, 'A' and 'B' from which indicator functions (I.F.) are constructed. Shown is the indicator function response for both A and B when odour A and B are presented. In each case the indicator function for the learnt odour is far higher than that for the distractor odour.

Hebbian learning was first applied to adapt the lateral weights of the network when exposed to Odour A and then applied a second time for 'Odour B'. After training, each odour ('Odour A' and 'Odour B') was presented sequentially for testing and the corresponding indicator functions for both learnt odours calculated over time (see Figure 5.6). We see that the corresponding indicator function for the learnt odour is high after a short time, whereas the other indicator function is low. When we present the second odour the situation is the opposite, indicating that the network is able to store two attractors corresponding to the two odours and we can read these out to classify the odours accordingly.

B. Odour Identification in Interfering Backgrounds

In order to test how robust the learnt odour classification scheme is in this case, we trained the system to a random pattern of steady-state activity across the array, which we termed 'Odour A' and used the network response to define the indicator function. When this input was presented, the pure Odour A stimulus gave rise to a large indicator function response, shown in Figure 5.7. In order to confound the input pattern, we then added different fractions of a random pattern, 'Odour B' to the original odour. In this case, the indicator function was found to reliably identify the presence of 'Odour A' even when the original learnt odour response was linearly superimposed on the distractor odour. To be sure that such a large indicator function response did not occur by chance or across all possible stimuli, Figure 5.7 also shows a low indicator function response in the trained network to a 3rd random odour input presented separately, 'Odour C'. Our demonstration of the ability of the network to solve this task corresponds to an important problem of identifying a learnt odour when presented in the context of some unknown, distractor, chemical such as in an explosives detection task.

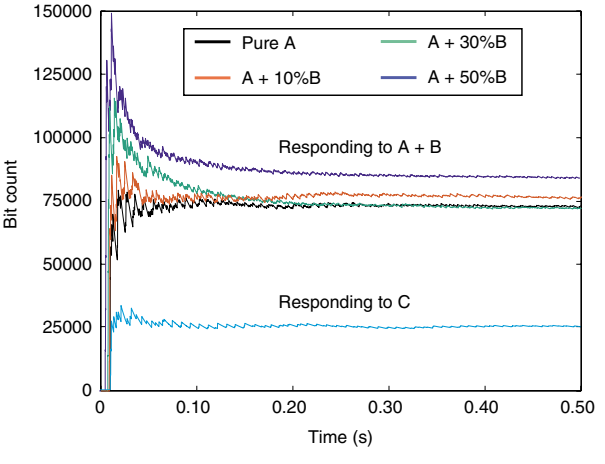

Fig. 5.7. Indicator functions for the odour identification in interfering background task. The network is trained to odour 'A' from which indicator function (I.F.) is constructed. Shown is the indicator function response for pure odour A and odour A mixed with various concentrations of a distractor odour B. Additionally, an odour C is applied to demonstrate low activity to untrained odours.

Such biologically-plausible networks will further be considered for their properties in complex odour detection tasks that have thus far not been solved using classical signal processing and pattern recognition approaches.

5.3.2 Spatiotemporal Information Measures

Fisher Information

In previous work we have discussed and analyzed how Fisher Information can be used to quantify the performance of an electronic nose (Sánchez-Montañés and Pearce 2001, Pearce and Sánchez-Montañés 2003). Basically, the *Fisher Information Matrix* (FIM) **F** is a square and symmetric matrix of $s \times s$ components, where s is the number of individual compounds whose concentration we are interested to estimate. In order to calculate **F** we should first calculate the individual FIMs for each sensor j:

$$\mathbf{F}_j = \int p(\mathbf{Y}_j \mid \mathbf{c}) \cdot \left[\frac{\partial p(\mathbf{Y}_j \mid \mathbf{c})}{\partial \mathbf{c}} \right] \cdot \left[\frac{\partial p(\mathbf{Y}_j \mid \mathbf{c})}{\partial \mathbf{c}} \right]^T \cdot d^L \mathbf{Y}_j \tag{5.5}$$

where $\mathbf{Y}_j$ is the response of sensor j and **c** is a vector with the concentrations of the s simple compounds. The equation is general in that the sensor response **Y** may either be a time-independent scalar or a time series vector (of dimension L). In this case the total FIM for the array is just the summation of the individual matrices for each sensor, $\mathbf{F}_j$. The probability distribution $p(\mathbf{Y}_j|\mathbf{c})$ represents the noisy response of the sensor to a given mixture with concentration vector **c** (odour space).

The usefulness of Fisher Information is given by the important property that the best square error across all unbiased techniques that use the noisy array responses to estimate the stimulus is (see Sánchez-Montañés and Pearce 2001 for discussion)

$$\varepsilon^2 = \text{trace}\,(\mathbf{F}^{-1}) \tag{5.6}$$

Importantly, the Fisher Information matrix **F** is closely related to the discrimination ability of the system, which is why we consider it in this context. For instance, it can be demonstrated that in a two-alternative forced choice discrimination between two stimuli (i.e. the system has to determine which of two possible complex odours $\mathbf{c}_1$ and $\mathbf{c}_2$ is being presented), the optimal probability of error $P(\epsilon)$ that can be achieved using linear sensors is $P(\epsilon) = 0.5 \cdot [1\text{-erf}(0.5 \cdot \lambda^{0.5})]$ with $\lambda \equiv \frac{1}{2} \cdot \delta\mathbf{c}^T \cdot \mathbf{F} \cdot \delta\mathbf{c}$ and $\delta\mathbf{c} \equiv \mathbf{c}_2\text{-}\mathbf{c}_1$.

In our previous work we have discussed how to calculate in practice this quantity when the temporal patterns of the responses of the individual sensors are not taken into account (corresponding to the first mechanism for discrimination identified in Section 1). Here we extend and calculate the Fisher Information for the spatiotemporal case which includes the role of time in the responses. The first step is to model the noise in the sensors, which will determine $p(\mathbf{Y}_j \mid \mathbf{c})$.

Dynamic Model of the Noise

Let us define $\mathbf{Y}_{j;\,\mathbf{c}}$ as the noisy temporal response (time series) of sensor j to stimulus **c**. $\mathbf{Y}_{j;\,\mathbf{c}}$ is a vector of L components (number of consecutive samples of the sensor). We will consider sensors with additive noise,

$$\mathbf{Y}_{j;\mathbf{c}} = \overline{\mathbf{Y}}_{j;\mathbf{c}} + \mathbf{n}_j \tag{5.7}$$

where $\overline{\mathbf{Y}}_{j;\mathbf{c}}$ is the expected time series response of sensor j to mixture **c**, and $\mathbf{n}_j$ is a noisy time series that corrupts the individual sensor response. Note that $\overline{\mathbf{Y}}_{j;\mathbf{c}}$ can be in principle a time series of arbitrary complexity, for instance a series with four different peaks. In order to calculate the Fisher Information we need to characterize the noise dynamics of $\mathbf{n}_j$. To first approximation, we model them as first-order AR processes, which we express in the convenient form

$$\mathbf{n}_j(k+1) = \gamma_j \cdot \mathbf{n}_j(k) + \sigma_j \cdot \sqrt{1-\gamma_j^{\,2}} \cdot \xi \tag{5.8}$$

with $k \in [1, L\text{-}1]$. Additionally, $\mathbf{n}_j(1)$ is modelled as a Gaussian random variable of zero mean and variance σ_j^2. In equation 6 and from now on we use parentheses to indicate the element of the vector (k) or matrix (u, v) to avoid confusion with subscripts. The coefficients γ_j and σ_j depend on each sensor; ξ is an I.I.D. Gaussian variable of unit variance and zero mean. Note that this implies that $\mathbf{n}_j$ has zero mean, variance σ_j^2 and auto-covariance given by:

$$\left\langle \mathbf{n}_j(k) \cdot \mathbf{n}_j(k+d) \right\rangle = \sigma_j^{\,2} \cdot \gamma_j^{|d|} \tag{5.9}$$

Therefore the noise vector $\mathbf{n}_j$ is a multivariate Gaussian process with zero mean and covariance matrix $\mathbf{N}_j$ given by

$$\mathbf{N}_j(u,v) = \sigma_j^{\,2} \cdot \gamma_j^{|u-v|} \tag{5.10}$$

where $u, v \in 1,\ldots,L$

Spatio-temporal Fisher Information

The expected time series response of a linear sensor j to a mixture **c** is given by (removing the constant sensor baseline):

$$\overline{\mathbf{Y}}_{j;\mathbf{c}} = \Sigma_i \, c_i \cdot \mathbf{A}_j^{\,i} \tag{5.11}$$

where $\mathbf{A}_j^{\,i}$ is the expected time series response of sensor j to a unit of concentration of single compound i. Equation 9 implies that the sensor response is linear to increasing concentration (within some reasonable limit) and to mixtures. We have found that this is a good approximation for the composite materials used in our artificial mucosa (data not shown).

Using the previous result that $\mathbf{Y}_{j;\,\mathbf{c}}$ is a Gaussian vector with covariance matrix $\mathbf{N}_j$, together with equation 3, it is straightforward to demonstrate

$$\mathbf{F}_j(u,v) = \left(\mathbf{A}_j^{\,u}\right) \cdot \mathbf{N}_j^{-1} \cdot \left(\mathbf{A}_j^{\,v}\right)^T \tag{5.12}$$

Using this equation together with equation 8 and using that sensors are causal ($\mathbf{A}_j(1, k) = 0$) we can derive after some algebra the following convenient equation

$$\mathbf{F}_j(u,v) = \frac{1}{\sigma_j^2 \cdot \left(1-\gamma_j^2\right)} \cdot \sum_{i=2}^{L} \mathbf{B}_j(i,u) \cdot \mathbf{B}_j(i,v) \tag{5.13}$$

with $\mathbf{B}_j(i, k) \equiv \mathbf{A}_j(i, k) - \gamma_j \cdot \mathbf{A}_j(i\text{-}1, k)$. This important equation represents the spatio-temporal Fisher Information of a noisy sensor within an array.

Purely Spatial Fisher Information

It is interesting to calculate how much better the spatio-temporal information is when compared to the information carried by sensor responses containing no explicit temporal information. Here we consider the contribution of the three mechanisms combined. In case that just the mean output of each sensor is used in subsequent signal processing:

$$y_{j;\mathbf{c}} = \frac{1}{L} \cdot \sum_{i=1}^{L} \mathbf{Y}_{j;\mathbf{c}}(i) \tag{5.14}$$

it is easy to demonstrate that this mean output is a Gaussian variable with average $\mathbf{a}_j^{\mathrm{T}} \cdot \mathbf{c}$, where

$$a_j(u) \equiv \frac{1}{L} \cdot \sum_{i=1}^{L} \mathbf{A}_j(i,u) \tag{5.15}$$

The variance of $y_{j;\mathbf{c}}$ can be calculated as:

$$\sigma_j^2\left(y_{j;\mathbf{c}}\right) = \frac{\sigma_j^2}{\left(1-\gamma_j\right)^2 \cdot L^2} \cdot \left[L - \gamma_j^2 L - 2\gamma_j\left(1-\gamma_j\right)\right] \tag{5.16}$$

Then the individual Fisher Information Matrices are given by (Sánchez-Montañés and Pearce 2001):

$$\mathbf{F}_j = \frac{1}{\sigma_j^2\left(y_{j;\mathbf{c}}\right)} \cdot \mathbf{a}_j \cdot \mathbf{a}_j^T \tag{5.17}$$

Fisher Information of the Microchannel to Mixtures of Toluene and Ethanol

The spatio-temporal Fisher Information Matrix was calculated for the micro-channel responding to toluene and ethanol odorants, such as that shown in Figure 5.3. Then the trace of the inverse of this matrix was calculated which corresponds to the optimal square error that any method estimating the individual concentrations could obtain.

Importantly, we see that the expected square error when using spatio-temporal information is always smaller than that error when only spatial information is considered (Figure 5.8). When using all the 16 available sensors in the array the ratio of the

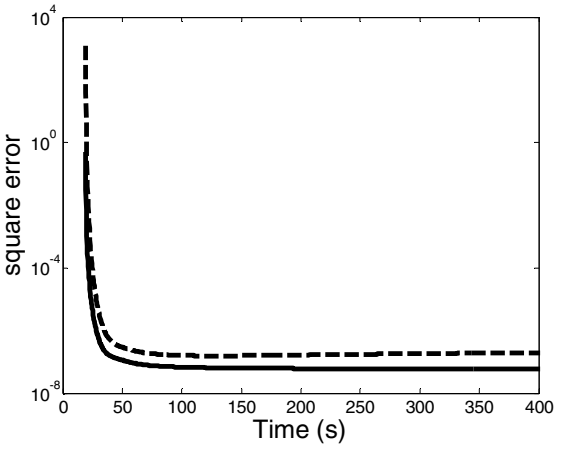

Fig. 5.8. Optimal square error in the estimation of the individual concentrations in mixtures of toluene and ethanol, as a function of the sampling time. All available sensors in the array are used. **Solid:** optimal square error $\epsilon^2_{\text{sp-temp}}$ when the spatial and temporal information in the sensor array is taken into account. **Dashed:** optimal square error ϵ^2_{sp} when only the spatial information is taken into account.

two square errors is 2.8. When the detection task is much harder, *i.e*. complex odours with large numbers of components, this ratio of the spatial error to spatio-temporal error is expected to be far higher.

In order to investigate more deeply how much improved the spatio-temporal information is with respect to pure spatial information (for the case of arbitrary mixtures of the two pure odours toluene and ethanol), we calculated the ratio of the two optimal estimation errors $\epsilon^2_{\text{sp-temp}}$ and ϵ^2_{sp} for all the 65,535 sets of sensors that can be generated out of our 16 available sensors (Table 5.1). Specifically, for each possible subset of sensors we have performed analogous calculations as those shown in Figure 5.8, and then computed the ratio of the minima of the two curves. Table 5.1 shows the resulting range of ratios for a given number of sensors.

Table 5.1. Range of the ratio $\epsilon^2_{\text{sp-temp}} : \epsilon^2_{\text{sp}}$ for all the possible combinations that can be generated out of our 16 available sensors

No. sensors	Improvement	No. sensors	Improvement
1	∞	9	1.6 – 50
2	1.5 – 860	10	1.7 – 33
3	1.4 – 580	11	1.7 – 18
4	1.4 – 370	12	1.8 – 5.8
5	1.5 – 270	13	2.1 – 3.9
6	1.5 – 170	14	2.2 – 3.5
7	1.5 – 83	15	2.3 – 3.1
8	1.6 – 72	16	2.8

For configurations with only one sensor, the ratio is always infinite since it is impossible to estimate the concentrations of the individual compounds from the average response of only one sensor, a task which on the other hand is possible to address when the temporal information is also considered. For small numbers of sensors the improvement of the performance of the system based on spatio-temporal information can be several orders of magnitude (Table 5.1), revealing that an artificial mucosa optimally designed for exploiting temporal features can increase largely the sensitivity as well as reduce the number of total sensors.

The important result of this analysis is that the spatiotemporal information available from a sensor time series can never be less than purely spatial information (such as the mean output over time). By increasing the diversity in the temporal responses the ratio of this information can be very high indeed, leading to large improvements in discrimination performance. The equations here characterise this explicitly in the linear case.

5.4 Conclusions

Achieving optimal detection performance in machine olfaction means exploiting both spatial and temporal sensor array responses, whereas traditionally only the spatial aspects have been employed. We have presented a new machine olfaction technology that demonstrates an additional mechanism for discrimination in these systems, which we have termed an artificial olfactory mucosa, on account of its similarities to biological odour delivery systems. The additional discrimination mechanism acts through the physical segregation in complex mixtures of odours combined with chemical sensor arrays that are distributed in space. Imposing spatio-temporal dynamics in the delivery of chemical components, we have shown, can confer additional diversity in the responses of chemosensor arrays which may form the basis of a new generation of electronic noses with improved sensitivity, discrimination performance and selectivity.

Taking advantage of this new sensing approach requires the consideration of both space and time during chemosensor array signal processing and classification. Here we have emphasised how a spiking implementation of the olfactory bulb, which is also biologically plausible, is able to learn and classify different olfactory inputs as well as identify particular odour stimuli present within a mixture of interfering distractor odorants.

More formally, a new information theory measure has been described which is capable of quantifying both spatial and temporal information in artificial mucosa based chemical sensor arrays. Importantly this analysis has demonstrated that the spatiotemporal case should outperform the purely spatial case emphasising the importance of time in these systems.

The artificial mucosa arrangement opens various possibilities for optimising both spatial and temporal response profiles to particular compounds and mixtures of interest – for instance by configuring sensor position. We are now applying this new information measure to the optimisation of artificial mucosa configurations to particular detection tasks which will uncover underlying design principles for making a new generation of complex odour detection devices with improved detection capabilities.

References

Albert, K.A., Gill, D.S., Walt, D.R., Pearce, T.C.: Optical Multi-bead Arrays for Simple and Complex Odour Discrimination. Analytical Chemistry 73, 2501–2508 (2001)

Amit, D.J.: Modeling Brain Function: The World of Attractor Neural Networks. Cambridge University Press, Cambridge (1992)

Brody, C., Hopfield, J.J.: Simple networks for spike timing computation and olfaction. Neuron. 37, 843–852 (2003)

Hildebrand, J.G., Shepherd, G.M.: Mechanisms of olfactory discrimination: converging evidence for common principles across phyla. Annu. Rev. Neurosci. 20, 595–631 (1997)

Gardner, J.W., Covington, J.A., Koickal, T.J., Hamilton, A., Tan, S.L., Pearce, T.C.: Towards an artificial human olfactory mucosa for improved odour classification. Proceedings of the Royal Society A: Mathematical, Physical and Engineering Sciences 463, 1713–1728 (2007)

Guerrero, R., Pearce, T.C.: Attractor-Based Pattern Classification in a Spiking FPGA Implementation of the Olfactory Bulb. In: Proceedings of the 3rd International IEEE EMBS Conference on Neural Engineering, Hawaii, USA (May 2007)

Guerrero-Rivera, R., Morrison, A., Diesmann, M., Pearce, T.C.: Programmable Logic Construction Kits for Hyper Real-time Neuronal Modeling. Neural Computation 18, 2651–2679 (2006)

Kepecs, A., Uchida, N., Mainen, Z.F.: The sniff as a unit of olfactory processing. Chemical Senses 31, 167–179 (2006)

Koickal, T.J., Hamilton, A., Tan, S.L., Covington, J.A., Gardner, J.W., Pearce, T.C.: Analog VLSI Circuit Implementation of an Adaptive Neuromorphic Olfaction Chip. IEEE Circuits and Systems 54, 60–73 (2007)

Li, Z., Dayan, P.: Computational differences between asymmetrical and symmetrical networks Network. Comput. Neural Syst. 10, 59–77 (1999)

Llobet, E., Brezmes, J., Vilanova, X., Sueiras, J.E., Correig, X.: Qualitative and quantitative analysis of volatile organic compounds using transient and steady-state responses of a thick-film tin oxide gas sensor array. Sensors and Actuators B - Chemical 41, 13–21 (1997)

Mori, K., Nagao, H., Yoshihara, Y.: The olfactory bulb: coding and processing of odour molecule information. Science 286, 711 (1999)

Pearce, T.C.: Computational Parallels between the Biological Olfactory Pathway and its Analogue The Electronic Nose: Part I Biological Olfaction. BioSystems 41, 43–67 (1997)

Pearce, T.C., Gardner, J.W., Nagle, H.T., Schiffman, S.S. (eds.): Handbook of Machine Olfaction. Wiley-VCH, Weinheim (2003)

Pearce, T.C., Sánchez-Montañés, M.A.: Chemical Sensor Array Optimization: Geometric and Theoretical Approaches. In: Handbook of Machine Olfaction: Electronic Nose Technology. In: Pearce, T.C., Schiffman, S.S., Nagle, H.T., Gardner, J.W. (eds.) Handbook of Machine Olfaction: Electronic Nose Technology, pp. 347–375. Wiley-VCH (2003)

Purnell, H.: Gas Chromatography. John Wiley & Sons, Chichester (1962)

Rubin, D.B., Cleland, T.A.: Dynamical mechanisms of odour processing in olfactory bulb mitral cells. J. Neurophysiol. 96(2), 555–568 (2006)

Sánchez-Montañés, M.A., Pearce, T.C.: Fisher Information and Optimal Odour Sensors. Neurocomputing 38, 335–341 (2001)

Schoenfeld, T.A., Cleland, T.A.: Anatomical contributions to odorant sampling and representation in rodents: zoning in on sniffing behavior. Chem. Senses 31, 131–144 (2006)

Wang, D.: Temporal pattern processing. In: Arbib, M. (ed.) The Handbook of Brain Theory and Neural Network, vol. 2, pp. 1163–1167. MIT Press, Cambridge (2003)

White, J., Kauer, J.S.: Odour recognition in an artificial nose by spatio-temporal processing using an olfactory neuronal network. Neurocomputing 26(7), 919–924 (1999)